FABAD J. Pharm. Sci., 49, 1, 163-180, 2024
Doi: 10.55262/fabadeczacilik.1346469
RESEARCH ARTICLE

Bilayer Nanofiber Scaffold Incorporated with Mupirocin and Thyme Essential Oil for Synergistic Activity Against Bacterial Wound Infections

Kisan JADHAV[*°], Shivani GHARAT [**], Shradha B. ADHALRAO[***]

Bilayer Nanofiber Scaffold Incorporated with Mupirocin and Thyme Essential Oil for Synergistic Activity Against Bacterial Wound Infections

SUMMARY

This study aimed to fabricate a bilayer nanofiber scaffold using an electrospinning process, incorporating a drug and oil-containing polymeric emulsion to enhance its effectiveness against bacterial wound infections. The research focused on characterizing the scaffold's morphology, chemical composition, thermal behavior, porosity, swelling ratio, drug release kinetics, in-vitro permeation, ex vivo skin permeation, and antimicrobial activity. Results from in-vitro drug permeation studies demonstrated an initial rapid release of Mupirocin (53% in 6 h) followed by sustained release (92.17% in 72 h). In comparison, Thyme Essential Oil exhibited a release profile with an initial burst followed by sustained release (85.45% release in 10 h). The ex vivo skin permeation data revealed greater permeability compared to conventional films; notably, the bilayer nanofiber scaffold exhibited superior antibacterial activity compared to single-layer Mupirocin and Thyme Essential Oil scaffolds, indicating a synergistic effect between Mupirocin and Thyme Essential Oil. This research offers an innovative approach to wound management with potential clinical implications.

Key Words: *Bilayer nanofiber scaffold, Wound infections, Mupirocin, synergistic activity, Thyme essential oil, Antibacterial activity.*

Bakteriyel Yara Enfeksiyonlarına Karşı Sinerjistik Aktivite için Mupirosin ve Kekik Uçucu Yağı ile Birleştirilmiş Çift Tabakalı Nanofiber İskele

ÖZ

Bu çalışma, bakteriyel yara enfeksiyonlarına karşı etkinliği arttırmak için bir ilaç ve yağ içeren polimerik emülsiyon içeren bir elektroeğirme işlemi kullanarak çift tabakalı bir nanofiber iskele üretmeyi amaçlamaktadır. Araştırma, iskelenin morfolojisini, kimyasal bileşimini, termal davranışını, porozitesini, şişme oranını, ilaç salım kinetiğini, in vitro permeasyonunu, ex vivo deri permeasyonunu ve antimikrobiyal aktivitesini karakterize etmeye odaklanmıştır. İn vitro ilaç permeasyon çalışmalarından elde edilen sonuçlara göre, Mupirosin başlangıçta hızlı bir salım (6 saatte %53) ve ardından sürekli salım (72 saatte %92,17) göstermiştir. Buna karşılık Kekik Esansiyel Yağı, sürekli salım (10 saatte %85,45 salım) ile devam eden bir ilk patlama etkisi ile salım profili sergilemiştir. Ex vivo cilt permeasyonu verileri, geleneksel filmlere kıyasla daha fazla geçirgenlik ortaya çıkarmıştır; özellikle, çift tabakalı nanofiber iskele, tek tabakalı Mupirosin ve Kekik Uçucu Yağı iskelelerine kıyasla üstün antibakteriyel aktivite sergilemiş ve bu, Mupirosin ve Kekik Uçucu Yağı arasında sinerjistik bir etki olduğunu göstermiştir. Bu araştırma, potansiyel klinik etkiler ile yara tedavisine yenilikçi bir yaklaşım sunmaktadır.

Anahtar Kelimeler: *Çift tabakalı nanofiber iskele, Yara enfeksiyonu, Mupirosin, sinerjistik aktivite, Kekik uçucu yağı, Antibakteriyel aktivite.*

Received: 19.08.2023
Revised: 17.01.2024
Accepted: 19.01.2024

[*] ORCID: 0000-0001-7563-3935, Department of Pharmaceutics, Bharati Vidyapeeth's College of Pharmacy, Sector 3A, CBD Belapur, Navi Mumbai-400614, Maharashtra. India.
[**] ORCID: 0000-0003-4972-8863, Department of Pharmaceutics, Bharati Vidyapeeth's College of Pharmacy, Sector 3A, CBD Belapur, Navi Mumbai-400614, Maharashtra. India.
[***] ORCID: 0000-0002-6065-1839,Department of Pharmaceutics, Bharati Vidyapeeth's College of Pharmacy, Sector 3A, CBD Belapur, Navi Mumbai-400614, Maharashtra. India.

[°] Corresponding Author; Dr. Kisan Jadhav
Email ID: krj24@rediffmail.com

INTRODUCTION

The presence of wounds is an inevitable part of patient care, and the risk of infection is a common concern in wound management. Currently, commercially available formulations of mupirocin, an antimicrobial agent commonly used in wound care, have shown effectiveness in preventing and treating infections. However, there is growing concern about the emergence of bacterial resistance to mupirocin, necessitating the exploration of alternative strategies to improve its efficacy (Alkilani et al., 2015).

In recent literature, nanofiber-based wound dressings have gained attention as a promising approach for delivering antimicrobial drugs. Nanofibers offer advantages such as a high surface area-to-volume ratio, increased porosity, and the ability to precisely control drug release. These attributes make them ideal for targeted drug delivery to wound sites while minimizing microbial penetration (Kamble et al., 2016).

Electrospinning, a widely employed technology for nanofiber production, offers ease of handling, precise control over fiber diameter, and cost-effectiveness. This method provides a platform to develop innovative wound dressings that can optimize drug release profiles and enhance therapeutic outcomes (Thenmozhi et al., 2017).

Mupirocin (MUP), a potent antimicrobial agent produced by the Gram-negative bacterium *Pseudomonas fluorescens*, has demonstrated effectiveness against various bacterial strains. However, it is essential to optimize its delivery to wounded tissues, as oral administration leads to the gradual breakdown of mupirocin into an inactive metabolite (Abbas et al., 2019).

Addressing the concern of mupirocin resistance, this study aims to formulate an electrospun bilayer nanofiber scaffold incorporating bothMupirocin and Thyme Essential Oil (TEO). The combination of these agents is expected to synergistically enhance their antibacterial effects, providing a potential solution to combat bacterial resistance and improve the therapeutic efficacy of wound care. Propolis and its combination with MUP against methicillin-resistant *Staphylococcus aureus* (MRSA) in nasal carriage of rabbits were found to result in a more profound reduction in bacterial cell count and inflammatory response (Onlen et al., 2007). Thyme Essential Oil (*Thymus vulgaris* L.), known for its natural antimicrobial properties and ability to reduce inflammation, holds promise as an adjunct to mupirocin in wound management (Rather et al., 2021).

In recent developments, MUP-loaded nanoemulsions have emerged as a promising solution for the treatment of superficial skin infections. These nanoemulsions, formulated with the inclusion of eucalyptus oil (EO), offer a novel approach to combat such infections effectively (Alhasso et al., 2023).

Moreover, for the management of invasive *Staphylococcus aureus* infections, a parenteral delivery system known as Nano-MUP has been devised. This innovative approach, involving liposome protection and enhanced drug delivery mechanisms, has shown remarkable improvements in antimicrobial efficacy, particularly within infected organs and Staphylococcus aureus-harboring phagocytic cells (Goldmann et al., 2019).

Furthermore, an important endeavor in this field has been the development of MUP nanoparticle-loaded hydrogel (MLH), with a primary focus on ensuring its biocompatibility for rat model wound healing and its safety for cell lines. Notably, the results have been promising, as evidenced by wound contraction, reduced secretion, increased development of new blood vessels, stimulation of hair follicle cells, and other wound healing indicators in burn wounds. In comparison to alternative treatment groups, MLH, and hydrogel have demonstrated superior performance in facilitating the healing process, marking a significant advancement in wound care strategies. These developments underscore the potential of Mupirocin formulations to revolutionize the treatment of skin

infections and wound management (Kamlungmak et al., 2021).

It's worth noting that commercially available Mupirocin formulations come in the form of creams and ointments, providing additional options for patients and healthcare providers in addressing skin infections (Bakkiyaraj et al., 2017).

In summary, this research focuses on developing an innovative electrospun bilayer nanofiber scaffold with MUP and TEO to address the challenge of bacterial resistance and improve the treatment of bacterial wound infections.

MATERIALS AND METHODS

Materials

Kawman Pharma Ltd. Mumbai, India. generously provided MUP. Polycaprolactone (Mn, 80,000) was purchased from Otto Chemie Pvt Ltd. Mumbai, India.The source of the Thymus vulgarisessential oil was Naturalis essential oil, India. Polyvinyl alcohol and Tween 80 were obtained from Research Lab Fine Chem Industries and Loba Chemie Pvt. Ltd. Respectively. Dichloromethane AR grade and Methanol AR grade were gainedfrom S.D. Fine Chemicals, Mumbai, India.The additional ingredients together with solvents belonging to analytical grade were utilized.

Preparation of MUP-PCL-TEO-PVA bilayer nanofiber scaffold

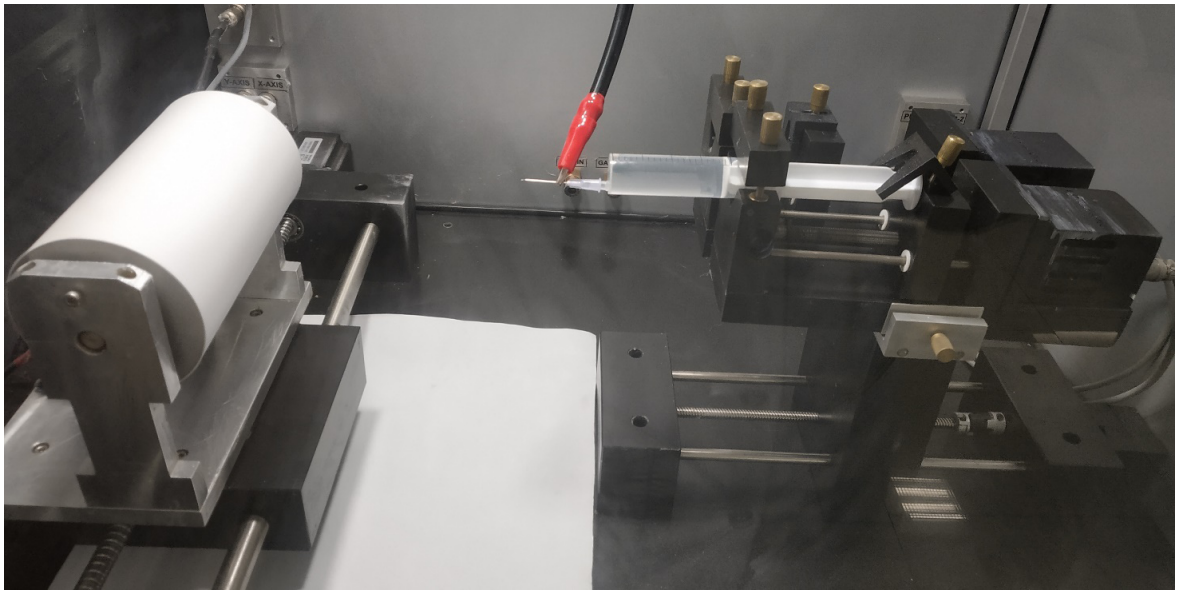

Figure 1. Electrospinning setup (E-SPIN NANO) for fabrication of MUP-PCL-TEO-PVA bilayer nanofiber scaffold.

Preparation of Electrospinning solutions

MUP-PCL polymeric solution

MUP-loaded PCL polymer solution was prepared based on a modified version of an existing technique (Chen et al., 2018). Using magnetic stirring, a precisely weighed amount of PCL was solubilized in DCM over 24 hours at room temperature, yielding a homogenous solution with a 10% (w/v) concentration. The PCL solution was then gradually added MUP (2 % w/v) while being vigorously stirred for 24 hours.

TEO- PVA loaded polymeric emulsion

To incorporate the oil in the polymeric solution, an o/w emulsion formulation was selected. The TEO-loaded emulsion was prepared by accurately weighing PVA (7% w/v) and dissolving in distilled water at 60-80°C along with 2 hours of constant magnetic stirring, to get a homogeneous solution. Then TEO (1% w/v) was dissolved in Tween 80 (3% w/v) and this oil-surfactant mixture was slowly added to the PVA solution (polymeric aqueous phase) and kept

nearly to 24 hours on magnetic stirring at room temperature to get a homogenous emulsion (KesiciGüler et al., 2019).

Preparation of bilayer nanofiber scaffold

The electrospinning technique for this investigation was carried out using the electrospinning device Espin Nano (as shown in Figure 1.). It consists of an adjustable DC power supply, a syringe, a stainless-steel needle, as well a syringe pump. The experimental criteria containing flow rate, supply voltage, tip-to-collector distance, as well as drum speed, were set based on previous literature as well as experimental conditions (Li et al., 2018). Processing for electrospinning was done at ambient temperature and 55% relative humidity. A syringe pump's flow rate was controlled using a 10 mL syringe having a 24-gauge metallic needle. The metal needle was charged using a high-voltage power source including an applied voltage of 18 kV, and on an aluminium foil-coated drum collector moving at 400–500 rpm, the fibers were collected. The flow rate was kept constant at 1 mL/h, and the tip-to-collector distance was set to 13 cm. For the preparation of bilayer nanofiber scaffolds, a first layer containing, TEO loaded PVA emulsion was deposited on aluminum foil followed by the second layer of MUP-loaded PCL solution. After that, a vacuum was applied to the fibers that had gathered from the aluminium foil upon the collector.

Gas Chromatography

The investigation employed an HP 6890 gas chromatography with a flame ionization detector (FID) and a 30 m x 0.25 mm HP-5 (cross-linked Phenyl-Methyl Siloxane) column with 0.25 µm film thickness from Agilent. The essential oil samples (0.1µL) were injected straight into the column. With a flow rate of 1, 4 mL min^{-1} and a split-less operation, helium was employed as the carrier gas. The column was kept at 40°C for five minutes, then elevated to 230°C at a rate of 10°C min^{-1}, and lastly from 230 to 280°C at a rate of 30°C min^{-1}.

Mass spectrometry analysis

A Hewlett Packard 6890 mass selective detector and a Hewlett Packard 6890 gas chromatograph were used to examine the oil using gas chromatography-mass spectrometry (GC-MS). The MS operating conditions were as follows: Ionisation potential is 70 Ev; ionization current, 2 A; ion source temperature is 200°C, and resolution is 1000. From 30 to 450 m/z, mass units were tracked. With retention indices related to n-alkanes.The chromatographic conditions were the same as those employed for GC analysis.

Characterization of electrospun MUP-PCL-TEO-PVA bilayer nanofiber scaffold

Scanning Electron Microscopy (SEM)

SEM was utilized for analyzing the surface morphological properties as well as the fiber diameter of electrospun nanofiber scaffolds.Using the FEI Quanta 200 SEM, nanofiber samples were imaged at varying magnifications after being gold-sputter-coated. At least 50 randomly chosen fibers were measured to estimate the fabrication's nanofiber membrane's average diameter.

Thickness

A Yuzuki digital micrometer was used to measure the nanofiber scaffold's thickness. Three samples() were measured at different areas of the nanofiber scaffold.

Porosity

The porous nature produced by the patches was measured using a procedure that has already been discussed. Absolute ethanol was used to immerse the scaffolds until they were saturated scaffolds were weighed before and after they had been soaked in alcohol. Porosity was measured using the equation given below:

Eq. (A.1):$P = P = \frac{W_2 - W_2}{\rho V_1} \times 100$

where W_1 and W_2 are the scaffolds' relative weights before and after being immersed in alcohol; V1 represents the volume previously immersed in

alcohol which was determined using the formula for the dressing's length, breadth, and height (Thakur et al., 2008).

Swelling ratio:

The nanofibrous scaffold was cut into equal portions and submerged in PBS (pH 7.4) for nearly 24 hours which represents medium conditions to gauge the level of swelling. After using filter paper to gently wipe away any water that had stuck to the surface, the scaffolds were promptly weighed.

Eq. (A.2): $DS = \frac{W_w - W_d}{W_d} \times 100$

In the above equation, DS stands for the amount of swelling, while W_w and W_d are the scaffolds' respective wet and dry weights (Tanrıverdi et al., 2018).

Fourier-transform infrared spectroscopy (FTIR)

A Fourier transform infrared spectrometer (SHIMADZU IR spirit) was utilized to get the infrared spectra of the electrospun scaffolds. After drying in a vacuum oven, nanofibrous mats were applied to the diamond crystal for investigation. The investigation included the spectral region from 4000 cm^{-1} to 400 cm^{-1}. For every spectrum, scans were recorded. To determine whether the formulation was causing any chemical interactions, the absorption peaks were examined.

Differential scanning calorimetry (DSC)

DSC (Hitachi 7020) was used to investigate thermal characteristics. As a reference, an empty aluminium pan was used. Using an aluminium sealed pan, DSC measurements were conducted from 10 to 300 °C at a heating rate of 10 °C/minute.Oil or Liquid holdingsample pans were used to characterize TEO. For each measurement, a sample size of 5–10 mg was used. During the measurement, nitrogen gas was used to purge the sample cell. In the context of DSC, melting refers to the process of a substance transitioning from a solid to a liquid state under the influence of increasing temperature.DSC measures the heat flow associated with the phase transition, allowing for the characterization of melting temperatures and enthalpies of materials.

% Entrapment efficiency (% EE)

To ascertain the % EE, the quantity of medication that was not trapped in the nanofibers was assessed. The nanofiber mat formed was diluted appropriately with methanol and then subjected to centrifugation for 30 minutes at 10,000 rpm.Utilizing a UV/VIS spectrophotometer with a wavelength of 230 nm, the quantity of free medicine in the supernatant was calculated. A similar process was followed to determine the TEO content at 274nm. The quantity of drug that was absorbed was determined by comparing the initial drug content with the free drug in the supernatant. The experiment was conducted in triplicate using three different samples.

***In vitro* drug release**

In vitro drug release of nanofiber scaffold was carried out as per described in the earlier method. By inserting a known mass and approximate size (4×4 cm^2) of material in 60 mL of PBS (pH=7.4) at 37° C, drug release from the MUP-loaded nanofiber scaffolds was assessed.1.0 mL of solution was moved to a sample vial from the test solution at predefined sample collection intervals. The amount of drug released was determined by a UV spectrometer (Shimadzu UV-1800) at a wavelength of 230 nm and the cumulative release percentage of MUP at various times was determined based on the calibration curve. TEO release was also detected using a UV spectrometer at 274 nm wavelength.

The amount of MUP and TEO released were calculated from:

Eq. (B.1): $y = 0.0243c + 0.0397$ ($R^2 = 0.995$)

where c is the concentration of MUP (mg/L) and y is absorbance.

Eq. (B.2): $y = 0.0606x - 0.0044$ ($R^2 = 0.996$)

where c is the concentration of TEO (mg/L) and y is absorbance.

***In vitro* drug permeation**

In vertical Franz diffusion cells, 22 ml of pH 7.4 phosphate-buffered saline (PBS) were added to the produced bilayer electrospun scaffolds (JN CIENCE-TECH).The complete scaffold was present in the diffusion cell's receptor chamber, which was below the sampling port.The scaffold showed promising wettability throughout the tests and maintained the entire immersion without any additional support. The interior compartments of the Franz cells were covered with cellulose membrane, while the outside jacket of the cells was kept at 37° C and agitated at 200 rpm. 1 ml of sample was taken out of the sampling port and replaced at the proper intervals between 1 and 72 hours with an equal volume of the new buffer. Shimadzu UV-1800 spectrometer was used to measure overall drug concentrations for MUP and TEO at wavelengths of 230 nm and 274 nm, respectively.

***Ex vivo* studies**

For the *ex vivo* study, a male white Wistar rat weighing 180–200 g was sacrificed by chloroform inhalation method. Abdominal hair was shaved off after scarification.The sample of injured tissue had the adherent fat and dirt thoroughly removed. Before beginning the diffusion studies, the skin sample was immersed in phosphate buffer saline solution for 30 min. [Approval statement: The above-mentioned project, "Bilayer Nanofiber Scaffold Incorporated with Mupirocin and Thyme Essential Oil for Synergistic Activity Against Bacterial Wound Infections." (Protocol No.-BVCP/IAEC/07/2020) consisting of male white Wistar rat has been reviewed and approved by the IAEC. Humane care of the obtained animal used in animal studies was done as per the IAEC guidelines].Vertical Franz diffusion cells with a diffusional surface area of 1 cm^2 and 32 ml of receptor cell volume were used for *ex vivo* permeation tests.First, the scaffold was fully submerged in the diffusion cell's receptor compartment underneath the sampling port.Second, a pH 7.4 phosphate buffered solution was added to the receptor compartments. The receptor phase was sustained at 37°C by employing a circulated water bath with stirring at 200 rpm. Diffusion barriers were made out of rat skin. Then, over 72 hours, 1 ml aliquots were regularly taken out and refilled with a similar amount of receptor fluid.This adequate further diluting of receiver contents was assessed with a UV spectrophotometer. The cumulative amount of drug permeated across the skin (ug/cm^2) was plotted against time (hr). The slope of the linear section of the graph was used to calculate the steady-state flux "J." Eq. 1 was used to calculate the Permeability Coefficient "Kp."

Eq. (C): $Kp = J/C_0$

Where C_0 is the drug concentration in the donor phase and J is the flux (Tas et al., 2007)

Antimicrobial studies

For antimicrobial assessment of electrospun nanofibers, the individual scaffolds of MUP-PCL, TEO-PVA, and combined bilayer scaffold of MUP-PCL-TEO-PVA was verified contrary to three microorganisms, *S. aureus*, *E. coli*, and *P. aeruginosa* using zone inhibitiontechniques to evaluate their antimicrobial action. Cultures of *S. aureus, E. coli, and P. aeruginosa* with a concentration of 108 CFU/ml were prepared on nutrient agar plates. A scaffold specimen with a diameter of 0.9 cm was positioned on top of a 100, l of 108 CFU/mL bacteria solution that had been spread out on an agar plate. Each sample's inhibitory region was quantified (Chen et al., 2017).

RESULTS AND DISCUSSION

Chemical composition of the essential oil

The output of essential oils was 1.0%. Freshly separated essential oil was a golden liquid with a strong, narcotic aroma. Sesquiterpene hydrocarbons, oxygenated sesquiterpenes, monoterpene hydrocarbons, and others were the five groups into which the constituents of essential oils were divided (Table 1). Thyme essential oil's GC and GC-MS analysis revealed 41 components, accounting for 97.85% of all detectable compounds. The main components of the oil were camphor (39.39%), camphene (17.57%),

α-pinene (9.55%), 1,8-cineole (5.57), borneol (5.03%), and β-pinene (4.32%). Less than 2% of other components were found overall (Table 1). The most significant monoterpene hydrocarbons, camphene, α-pinene,β-pinene, and myrcene, were present in thyme essential oil. The oil's most prevalent component class (54.82%) was oxygenated monoterpenes.

Table 1. Chemical composition of the essential oil.

Compound	Content %	Compound	Content %
Tricyclene	0.64	Terpinene-4-ol	2.21
Alpha-thyjene	0.46	Para-cymen-8-ol	0.28
Alpha pinene	9.35	Alpha terpineol	0.57
Camphene	17.19	Verbenone	0.13
Beta pinene	4.23	Carveol 1	0.22
Myrcene	3.21	Carvarcrol methyl ethyl	0.11
Alpha terpinen	0.27	Bornyl acetate	0.40
Para cymene	1.19	Thymol	0.24
1,8-cineole	5.45	Alpha-copaene	0.30
Trans Beta ocimene	0.09	Beta-bourbonene	0.12
Gama terpinene	0.55	Alpha-Gurjunene	0.66
Cis-sabinene hydrate	0.46	Beta-caryophyllene	0.09
Camphenilone	0.31	Aromadendrene	0.11
Alpha-terpinolene	0.11	Alpha-elemene	0.22
Linalol	0.14	Germacrene-d	0.23
Alpha-thyjone	0.29	Bicyclogermacrene	0.13
Neoalloocimene	0.53	Spathulenol	0.73
Camphor	38.54	Caryophellene oxide	0.56
Borneol	4.92	Beta-oplepenone	0.07

Scanning Electron Microscopy (SEM)

SEM was used to validate the creation of nanofibers. SEM images revealed the development of casually oriented uniform and homogeneous fibers having a diameter range of 325–419 nm. It is assumed that the drug was encapsulated and molecularly disseminated within the electrospun fibers because the photos did not indicate the existence of the drug crystals and/or aggregates on the surface (Figure 2.)(Kamble et al., 2016).

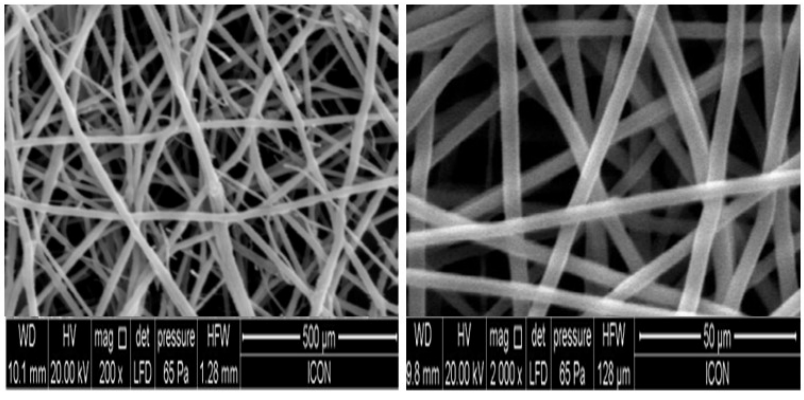

Figure 2. SEM images of electrospun MUP-PCL-TEO-PVA bilayer nanofiber scaffold.

Thickness

The thickness of nanofiber scaffold was confirmed by utilizing Yuzuki digital micrometer. Three samples were measured which give thickness 107 μm ,109 μm, and 113 μmrespectively which shows the optimum thickness of nanofiber scaffold attributed to the ideal wound dressing material. The number of nanofibrous layers that cover each other increases as the thickness of nanofibrous scaffolds does, which causes a reduction in air permeability and an enhancement in the compaction and tightness of the nanocomposite scaffold (Ghasemi-Mobarakeh et al., 2009).

Porosity

The porosity of the MUP-PCL-TEO-PVA bilayer nanofiber scaffold by the alcohol immersion method was found to be 82% which indicates good porosity. Electrospinning creates scaffolds with a greater porosity compared to previous techniques (Li et al., 2019). A bacterial wound dressing benefits from the scaffolds' high porosity, which helps to promote hydration and prevent infection (Li et al., 2018).The highly porous nature of the patches may assist in removing discharge from the injury site as well as avoid wound infection. Additionally, the great amount of porous nature present acts as an advantage in delivering nutrients and O_2 to the cells connected to the dressings (Liang et al., 2016).

Swelling ratio

A gravimetric approach was used to determine the swelling index of electrospun nanofiber materials. The loading and release behavior of medication is significantly influenced by the nanofibers' swelling index. The degree of swelling of MUP-PCL-TEO-PVA scaffolds in PBS pH 7.4 after 24 h was 257.43%. However, after maximum swelling (351.57%) was noted at 12 h.In all cases, additional extensions of time revealed a reduction in the intensity of edema. This decline in inflammation is mostly because of the breakdown of polymers, which causes the leakage of polymer from the nanofiber patch and reduces edema.The nanofibers' strong hydrophilicity and excellent swelling capabilities allow them to collect exudates at the wound site and keep it moist.

FTIR

The physical and chemical interactions of the polymers were studied using FTIR spectroscopy. The spectra of the MUP-PCL-TEO-PVA bilayer nanofiber scaffold exhibited preservation of all the characteristic bands (Figure 3a). Due to the lack of any chemical interaction, there was also no significant shifting of the existing bands or the emergence of new bands, indicating the compatibility of all nanofiber scaffold components. From the above overlay plot (Figure 3b.) of a pure drug (MUP), PCL, PVA, TEO, TWEEN 80, and nanofibers scaffold it has been observed that the medicine and the excipients utilized do not physically interact.

In the comprehensive FTIR analysis, the spectra of a film formulation containing the drug MUP alongside excipients such as PCL, PVA, TWEEN80 along TEO, were meticulously examined. By comparing these spectra with the isolated peaks of the drug MUP, a noteworthy revelation was observed. The distinct peaks corresponding to C-H Bending (806.14 cm^{-1}), CO-O-CO Stretching (1044.04 cm^{-1}), C-O Stretching (1143.17 cm^{-1}), C-N Stretching (1221.62 cm^{-1}), N-H Bending (1469.79 cm^{-1}), and C=C Stretching (1653.78 cm^{-1}) in drug MUP were found to be harmoniously echoed in the formulation's spectra. Furthermore, the presence of specific peaks associated with TEO and PCL within the formulation was also noted. This compelling evidence collectively suggests that there is no discernible interaction between the drug MUP and the selected excipients, thus affirming the compatibility of the drug with the formulation components.

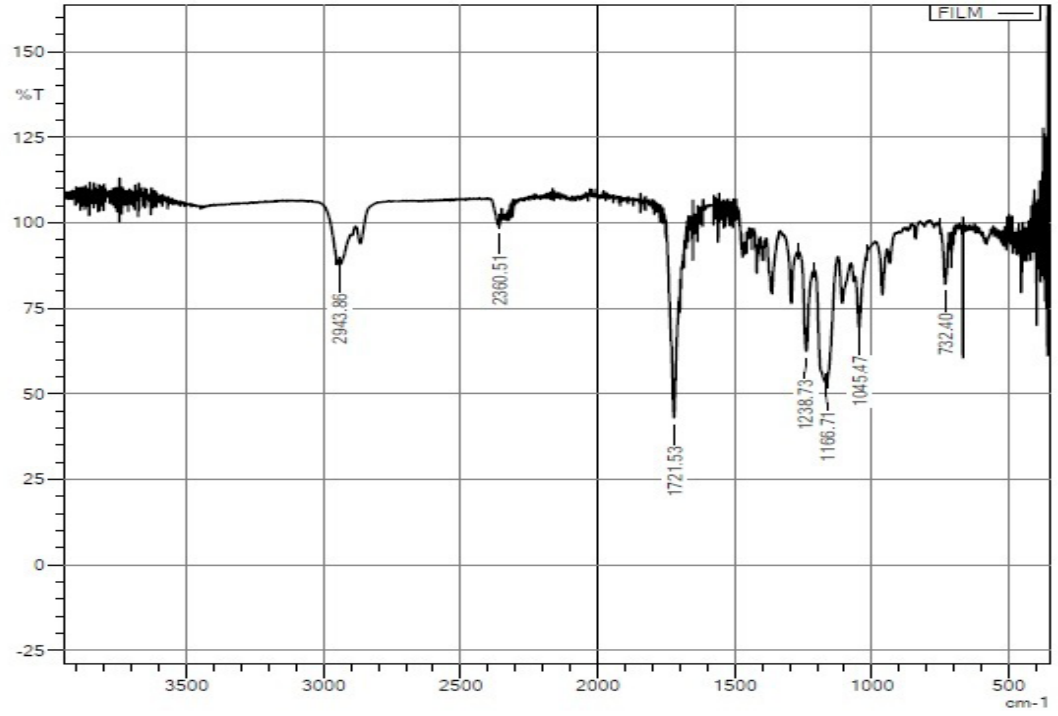

Figure 3a. FTIR spectra of MUP-PCL-TEO-PVA bilayer nanofiber scaffold.

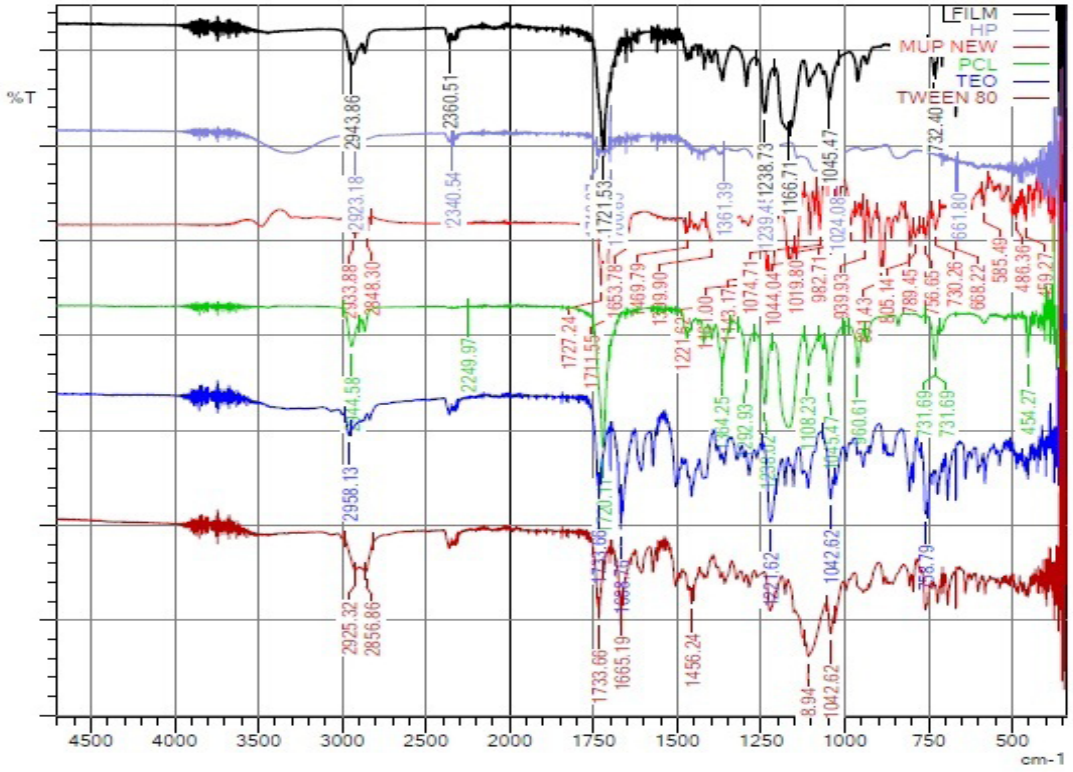

Figure 3b. Overlay plot of the pure drug (MUP), PCL, PVA, TEO, and TWEEN 80.

DSC

DSC is a technique for determining the temperature and energy variations associated with a compound's phase transitions, which aids in determining the degree of crystallinity.The crystalline character of MUP was confirmed by its abrupt endothermic peak at 71.5°C, which corresponds to its melting point Figure 4a. Also, TEO oil exhibited an endothermic peak at 215°C (Figure 4b). The DSC thermogram of both the polymer used in formulation i.e., PCL shows endothermic peaks at 57.7°C and PVA shows endothermic peaks at 192.7°C respectively. However, the MUP-PCL-TEO-PVA bilayer nanofiber scaffold showed an endothermic peak only at 53.3°C and 193.0°C for two polymers PCL and PVA respectively as shown in (Figure 4c) whereas, peaks associated with MUP and TEO melting points were not present which indicates the whole amorphization and solubilization respectively when nanofibers formulations were prepared.

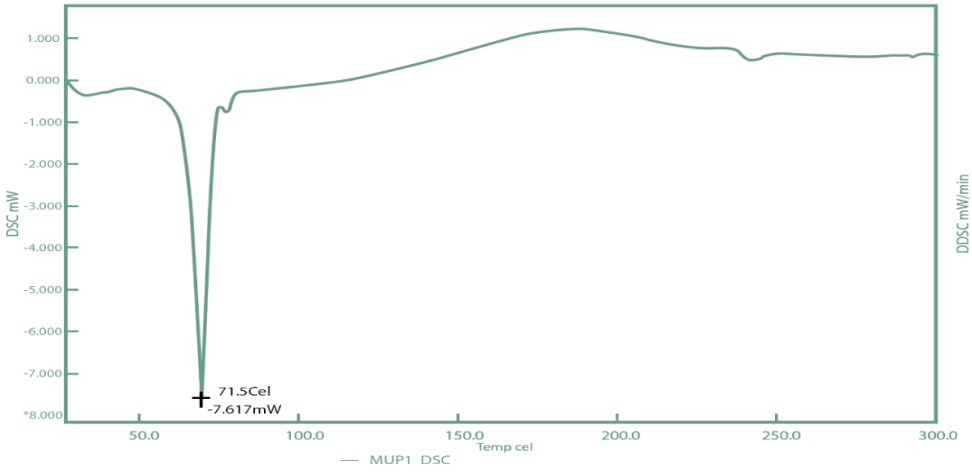

Figure 4a. DSC thermogram of pure MUP.

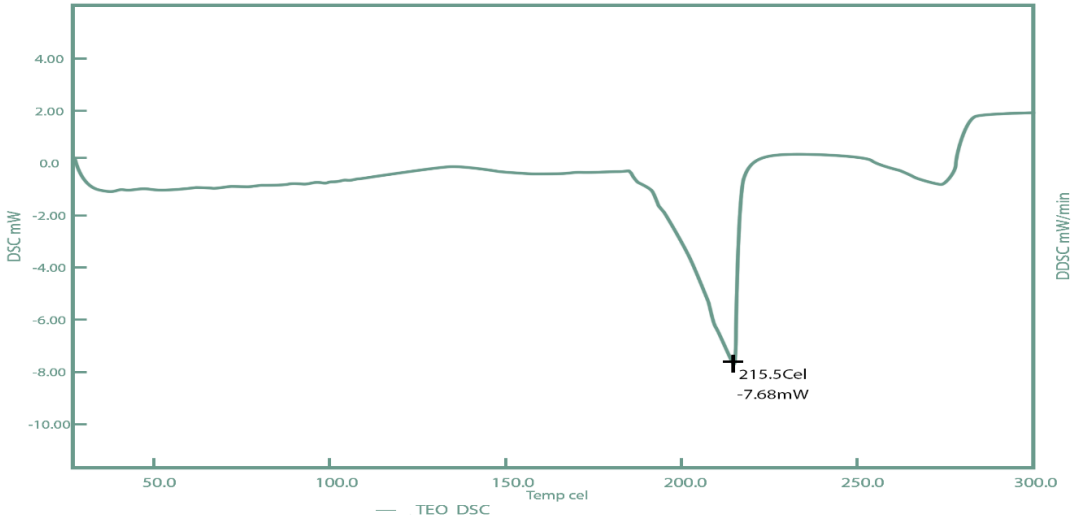

Figure 4b. DSC thermogram of TEO.

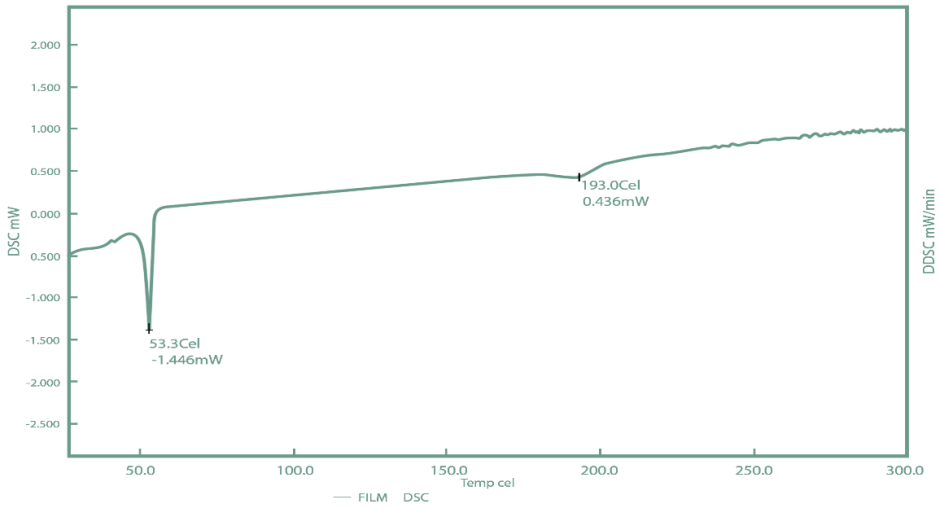

Figure 4c. Thermogram of MUP-PCL-TEO-PVA bilayer nanofiber scaffold

% Entrapment efficiency (% EE)

The % EE of the final optimized batch of bilayer nanofiber scaffold of MUP-PCL-TEO-PVA was studied using the UV spectroscopic method. The %EE of bilayer nanofiber scaffold was found to be 97.39 % and 93.06 % respectively for MUP and TEO.

***In vitro* drug release**

The drug release profiles of an optimized batch from the MUP-PCL-TEO-PVA bilayer nanofiber scaffold are illustrated in Figure 5. The calibration curves of MUP at 230 nm were R^2 = 0.995 and TEO at 274 nm was R^2 = 0.9961. MUP displayed a prolonged release from the bilayer nanofiber scaffold for 3 days. A two-stage release profile initially showed rapid release and thereafter showed a slower sustained release. Figure 5 displays the results of a sustained release profile of MUP from the Bilayer nanofiber scaffold for 3 days. The initial rapid release of MUP from the bilayer nanofiber scaffold resulted in the release of 40.55% of the total MUP content in the first 6 hours. With the sustained release, another approximately 53% was released from the bilayer scaffold in the following 72 hours.TEO exhibited a two-stage release, initially showed rapid release, and thereafter slower sustained release was observed. About 48% of TEO was released from the bilayer nanofiber scaffold in the first hours. The cumulative drug release increased steadily to 87% in the following 10 hours.

Though identical drug release profiles could be seen for MUP as well as TEO, 49% of the TEO exhibited burst release during the first hour, whereas 27% of the MUP dispersedout of the nanofiber scaffold simultaneously. This was explained by the fact thatintense chemical linkage bonds of PCL and MUP conjugated to the fiber, resulted in a lower release ability of MUP in comparisonto TEO. Thyme essential oil with a burst release profile can quickly reduce the microbial load in the wound, promoting faster wound healing by creating a more favorable environment for tissue repair. MUP, while slower to release, can provide a sustained antimicrobial effect, ensuring continuous inhibition of microbes even after the initial rapid action of thyme essential oil. The combined action of both agents can be effective in addressing both the immediate need for rapid microbial reduction and the longer-term need for sustained antimicrobial activity, ultimately contributing to improved wound healing outcomes. Drug release from the bilayer nanofiber scaffolds is dependent on the concentration of polymers used and the flow rate of polymeric solutions for electrospinning. This means polymers with a smaller size range with a larger interfacial area, thus promoting the controlled release of the drug from the formulation. Multiple options for controlling release time profiles are available with electrospun medicated fibers having a multilayer structure.

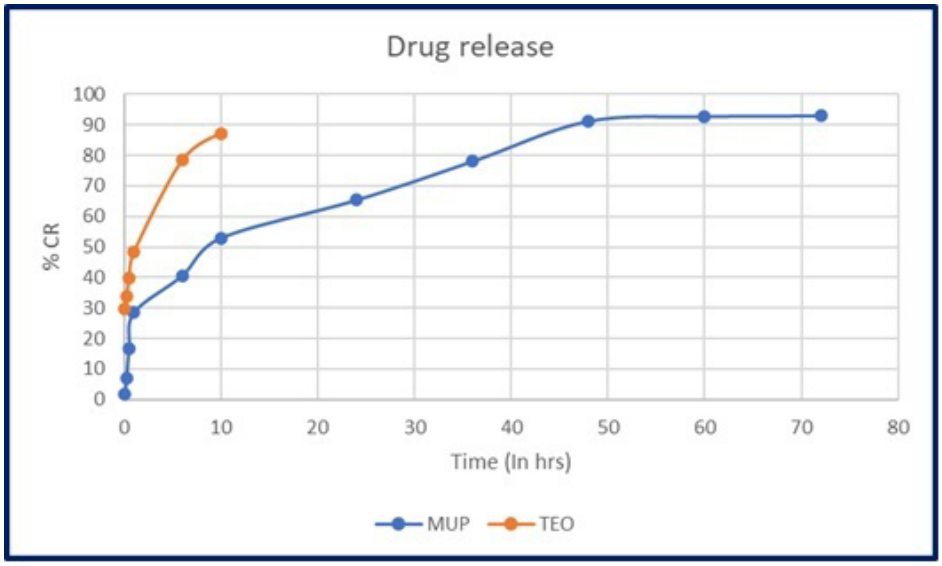

Figure 5. *In vitro* drug release of MUP and TEO from the MUP-PCL-TEO-PVA bilayer nanofiber scaffold.

***In vitro* drug permeation**

The *in vitro* drug permeation study of the MUP-PCL-TEO-PVA bilayer nanofiber scaffold was conducted using a Franz diffusion cellfor 72 h. The drug permeation study was conducted for 72 hours. From acquired results (Figure 6), it was found that MUP showed initial rapid release and thereafter a slower sustained releaseachieving 92.17% drug release after 72 h whereas TEO showed 85.45% release in 10 h with initial burst release and thereafter a sustained release profile. *In vitro*, drug permeation studies interpret the diffusion-derived drug delivery from nanofiber scaffold by following the KorsmeyerPeppas plot.

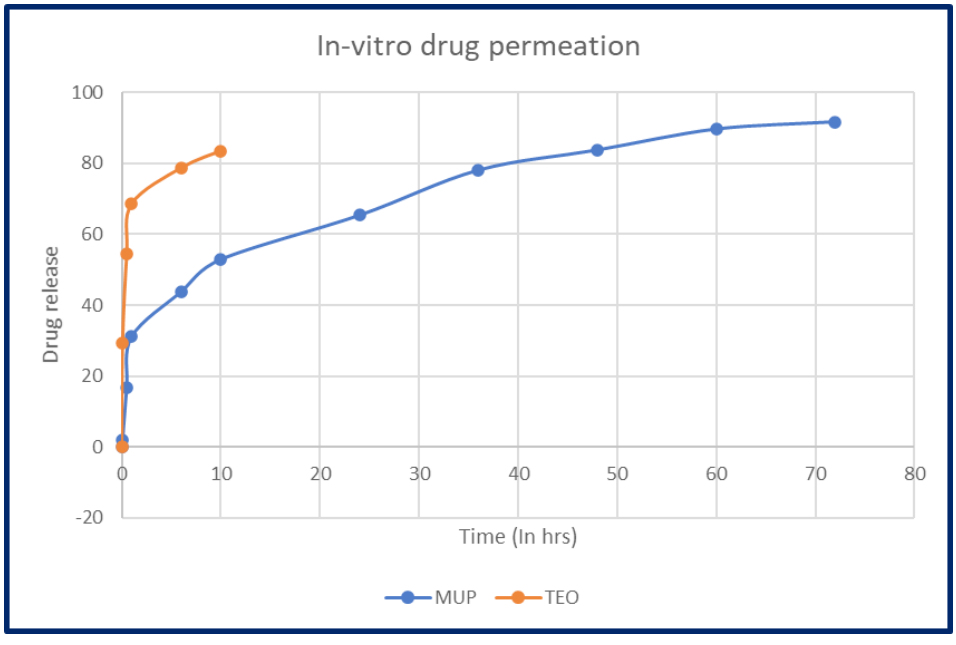

Figure 6. *In vitro* drug permeation of MUP and TEO from the MUP-PCL-TEO-PVA bilayer nanofiber scaffold.

Ex vivo studies

The *ex vivo* skin permeation study was performed by utilizing Franz diffusion cell for the MUP-PCL-TEO-PVA bilayer nanofiber scaffold. Here the skin is not whole in injured tissue. The study was carried out for 72 hours. From the results, it was found that MUP showed initial rapid release followed by a slower sustained release achieving 91.67% of drug release whereas TEO showed 83.45% release in 10 h with initial burst release followed by sustained release profile (Figure 7). The *ex vivo* skin permeation data displayed that for the MUP-PCL-TEO-PVA bilayer nanofiber scaffold the flux of nanofiber mats was found to be 5.12 and permeability was found to be 0.00425 which is greater than that of conventional cast film. BVCP/IAEC/07/2020 is the proposal no. for *ex vivo* studies.

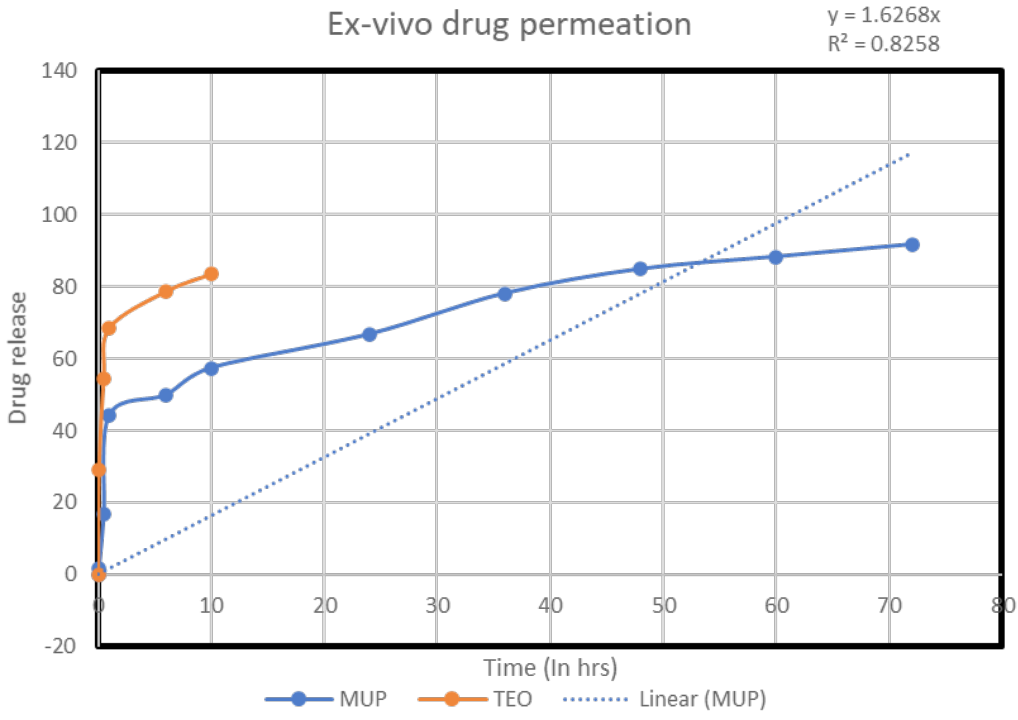

Figure 7. *Ex vivo* skin permeation from MUP-PCL-TEO-PVA bilayer nanofiber scaffold.

Antimicrobial studies

Antibacterial activity of individual scaffolds of MUP-PCL, TEO-PVA, and combined bilayer scaffold of MUP-PCL-TEO-PVA was verifiedin contrast to3 microorganisms, *S. aureus*, *E. coli*, and *P. aeruginosa* to evaluate their antimicrobial action. The inhibitoryregionformed by the respective sample was evaluated. Figure 8 shows the activity of MUP-PCL, TEO-PVA, and combined bilayer scaffold. Zone of inhibition for *S. aureus* was shown as 17 mm, 11 mm, and 21 mm by MUP alone, TEO alone, and bilayer MUP-PCL-TEO-PVA respectively. The activity of MUP-PCL, TEO-PVA, and combined bilayer scaffold for *P. aeruginosa,* shows the inhibitory region as 14 mm, 8 mm, and 17 mmrespectively. The activity of MUP-PCL, TEO-PVA and combined bilayer scaffold for *E. coli* shows the inhibitory region as 11 mm, 6 mm, and 12 mm respectively.

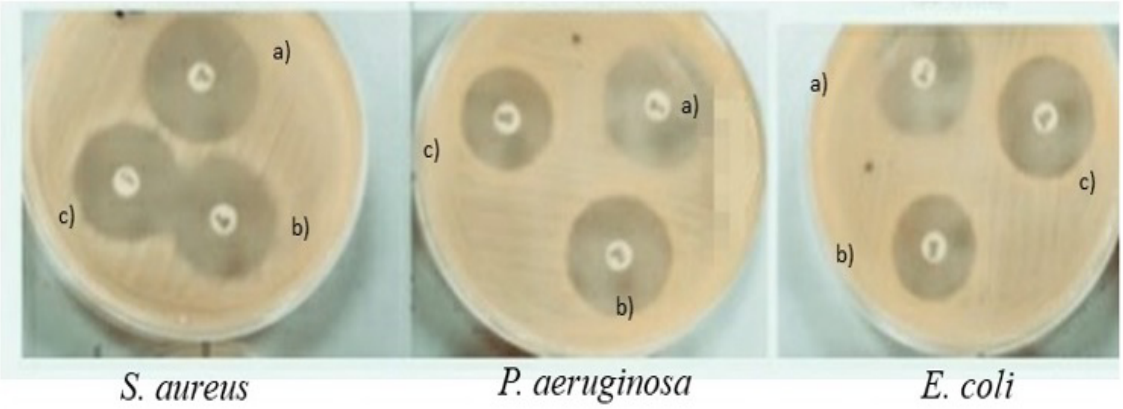

Figure 8. Antibacterial activity of MUP-PCL-TEO-PVA bilayer nanofiber scaffold against *S. aureus*, *P. aeruginosa,* and *E. coli*. [(a) MUP-PCL-TEO-PVA bilayer nanofiber scaffold, (b) MUP+PCL scaffold, (c) TEO+ PVA scaffold]

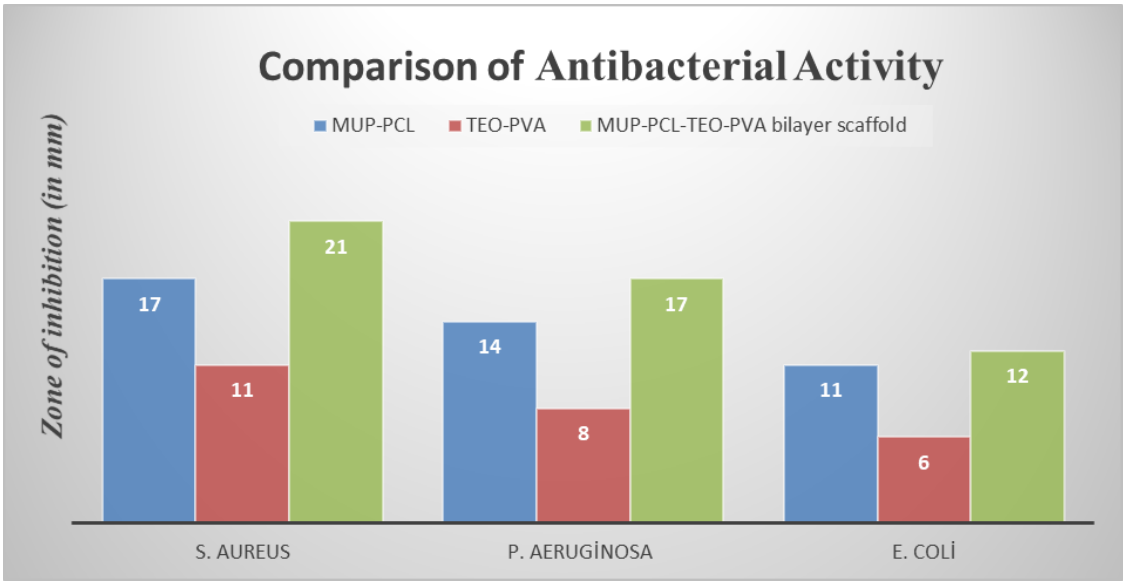

Figure 9. Statisticalrepresentationcomparing the antibacterial activity of MUP-PCL-TEO-PVA bilayer nanofiber scaffold against *S. aureus*, *P. aeruginosa,* and *E. coli*. [(a) MUP-PCL-TEO-PVA bilayer nanofiber scaffold, (b) MUP+PCL scaffold, (c) TEO+ PVA scaffold]

The bilayer MUP-PCL-TEO-PVA scaffold exhibitedoutstandingactionin contrast to all tested microorganisms, through the toughest action counter to *S. aureus* (21 mm), following this with *P. aeruginosa* (17 mm), and lastly*E. coli* (12 mm).Generally, this bilayer nanofiber scaffold displayed noteworthy action contrary to *S. aureus*, *E. coli*, as well as *P. aeruginosa.* The comparison is showcased in the Figure 9. To determine whether the observed differences in antibacterial activity are statistically significant, a one-way ANOVA was conducted followed by Tukey's Honestly Significant Difference test (post hoc Analysis). Based on the post hoc analysis, the comparison between MUP-PCL and TEO-PVA has a p-value of 0.08, which is not statistically significant ($p > 0.05$). However, the comparisons between MUP-PCL-TEO-PVA and both MUP-PCL ($p = 0.02$) and TEO-PVA ($p = 0.04$) are statistically significant ($p < 0.05$). In this scenario, it

concludes that MUP-PCL-TEO-PVA has the highest antibacterial efficacy among the tested scaffolds.Thus, the scaffold produced here possibly will increase efficacy in treating bacterial-infected injuries due to the combined antibacterial effect of MUP and TEO. Mupirocin is a potent antibacterial agent and is extensively utilized by medical practitioners as a topical ointment to cure various topical wounds MUP acts in contrast to a wide range of bacteria by resisting bacterial protein and RNA production by reversibly blocking isoleucyl-transfer RNA (Perumal et al., 2014).

CONCLUSION

In conclusion, this study successfully fabricated a novel MUP-PCL-TEO-PVA bilayer nanofiber scaffold using the electrospinning technique. The choice of polymer concentrations and electrospinning parameters played a critical role in determining drug release, % EE, and nanofiber structure. Notably, nanofibers composed of 10% PCL and 7% PVA exhibited favourable % EE and controlled drug release properties.

Characterization studies, including FTIR and DSC analyses, provided compelling evidence of the successful incorporation of both MUP and TEO within the nanofiber matrix. Furthermore, SEM images confirmed the formation of uniform and homogeneous nanofibers, essential for their efficacy as wound dressings.

In vitro drug permeation studies revealed distinct release profiles for MUP and TEO, with MUP initially displaying a rapid release followed by sustained drug release over 72 hours. Conversely, TEO exhibited an initial burst release followed by a sustained release pattern, reaching a significant level of release within 10 hours. This differential release kinetics could offer a tailored approach to wound treatment, allowing for rapid antimicrobial action (MUP) alongside longer-lasting benefits (TEO).

The *ex vivo* skin permeation data demonstrated that the MUP-PCL-TEO-PVA bilayer nanofiber scaffold exhibited superior permeability compared to conventional cast films, indicating its potential for improved transdermal drug delivery.

Most importantly, the antibacterial activity assessment highlighted the synergistic effect of MUP and TEO within the bilayer nanofiber scaffold. The increased zone of inhibition observed in the MUP-PCL-TEO-PVA bilayer scaffold, as compared to single-layer MUP and TEO scaffolds, underscores the potential of this innovative approach in combating bacterial infections more effectively.

Overall, our study offers a promising avenue for advanced wound care through the development of a bilayer nanofiber scaffold that combines the strengths of MUP and Thyme Essential Oil, potentially reducing bacterial resistance and improving treatment outcomes for bacterial wound infections.

ACKNOWLEDGEMENTS

This work was supported by AICTE by providing financial support under the Research Promotion Scheme (File No. 8-4/RIFD/RPS/policy-1/2017-2018) for the purchase of ESPIN NANO equipment and chemicals to carry out the research work. We are immensely grateful to Kawman Pharma Ltd. Mumbai, India, for providing the sample of MUP.

CONFLICT OF INTEREST

Authors declare that there is no conflict of interest.

AUTHOR CONTRIBUTION STATEMENT

In the collaborative endeavour of developing the mupirocin and thyme essential oil bilayer nanofiber scaffold for synergistic activity against bacterial wound infections, each author played a distinctive

role, contributing to various aspects of the research. Author Dr. Kisan JADHAV was instrumental in formulating the initial hypothesis, laying the foundation for our investigation. Shivani GHARAT actively engaged in the experimental design and execution, overseeing the intricate process of scaffold development. Simultaneously, Shradha ADHALRAO took charge of preparing the study text, ensuring clarity and coherence in presenting our findings. All authors collaborated in reviewing the text, collectively refining the manuscript to meet rigorous scientific standards. Statistical analysis and interpretation of the data were meticulously conducted by Shivani GHARAT, utilizing advanced methodologies to derive meaningful conclusions. Shradha ADHALRAO spearheaded the extensive literature research, grounding our work in existing knowledge and identifying gaps in understanding. The collaborative effort extended to critical discussions and consensus-building throughout the research journey, ultimately culminating in a comprehensive and impactful contribution from each author to the successful completion of this study.

REFERENCES

Alkilani A.Z.,McCrudden M.T.C., Donnelly R.F. (2015). Transdermal drug delivery: Innovative pharmaceutical developments based on disruption of the barrier properties of the stratum corneum. Pharmaceutics,7, 438–470. https://doi.org/10.3390/pharmaceutics7040438.

Abbas M., Hussain T., Arshad M., Ansari A.R., Irshad A., Nisar J. (2019). Wound healing potential of curcumin cross-linked chitosan/polyvinyl alcohol. International Journal of Biological Macromolecules,140, 871–876. https://doi.org/10.1016/j.ijbiomac.2019.08.153

Alhasso B., Ghori M.U., Conway B.R. (2023).Development of Nanoemulsions for Topical Application of Mupirocin, Pharmaceutics, 15(2), 378-380. https://doi.org/10.3390/pharmaceutics15020378

Bakkiyaraj D., Sritharadol R., Padmavathi A.R., Nakpheng T., Srichana T. (2017). Anti-biofilm properties of a mupirocin spray formulation against Escherichia coli wound infections,Biofouling, 33, 591–600. https://doi.org/10.1080/08927014.2017.1337100.

Chen X., Zhao R., Wang X., Li X., Peng F., Jin Z.(2017). Electrospunmupirocin loaded polyurethane fiber mats for anti-infection burn wound dressing application. Journal of Biomaterials Science, Polymer Edition, 28, 162–176. https://doi.org/10.1080/09205063.2016.1262158.

Ghasemi-Mobarakeh L., Morshed M., Karbalaie K., Fesharaki M.A., Nematallahi M., Nasr-Esfahani M.H. (2009). The thickness of electrospun poly (ε-caprolactone) nanofibrous scaffolds influences cell proliferation, 32, 679-689. ttps://doi.org/10.1177/03913988090320030

Goldmann O., Cern A., Müsken M., Rohde M., Weiss W., Barenholz Y. (2019). Liposomal mupirocin holds promise for systemic treatment of invasive Staphylococcus aureus infections. Journal of Controlled Release, 316, 292–301. https://doi.org/10.1016/j.jconrel.2019.11.007

Kamble R.N., Gaikwad S., Maske A., Patil S.S. (2016). Fabrication of electrospunnanofibers of BCS II drug for enhanced dissolution and permeation across skin. Journal of Advanced Research,7, 483–489. https://doi.org/10.1016/j.jare.2016.03.009.

Kamlungmak S., Nakpheng T., Kaewpaiboon S., Bintang MAKM., Prom-in S., ChunhachaichanaC. (2021).Safety and Biocompatibility of Mupirocin Nanoparticle-Loaded Hydrogel on Burn Wound in Rat Model. Biological and Pharmaceutical Bulletin, 44(11), 1707–1716. https://doi.org/10.1248/bpb.b21-00397

KesiciGüler H., Cengiz C.F., SesliÇetin E. (2019). Antibacterial PVP/cinnamon essential oil nanofibers by emulsion electrospinning. Journal of the Textile Institute, 110, 302–310. https://doi.org/10.1080/00405000.2018.1477237.

Liang D., Lu Z., Yang H., Gao J., Chen R. (2016). Novel Asymmetric Wettable AgNPs/Chitosan Wound Dressing: In Vitro and in Vivo Evaluation. ACS Applied Materials and Interfaces, 8, 3958–3968. https://doi.org/10.1021/acsami.5b11160.

Li J., Zhou Y., Yang J., Ye R., Gao J., Ren L. (2019). Fabrication of gradient porous microneedle array by modified hot embossing for transdermal drug delivery. Materials Science and Engineering C, 96, 576–582. https://doi.org/10.1016/j.msec.2018.11.074.

Li X., Wang C., Yang S., Liu P., Zhang B. (2018). Electrospun PCL/mupirocin and chitosan/ lidocaine hydrochloride multifunctional double layer nanofibrous scaffolds for wound dressing applications. International Journal of Nanomedicine, 13, 5287–5299. https://doi.org/10.2147/IJN.S177256.

Onlen Y., Duran N., Atik E., Savas L., Altug E., Yakan S. (2007). Antibacterial activity of propolis against MRSA and synergism with topical mupirocin. Journal of Alternative and Complementary Medicine, 13, 713–718. https://doi.org/10.1089/acm.2007.7021.

Perumal S., Ramadass S.K., Madhan B. (2014) Sol-gel processed mupirocin silica microspheres loaded collagen scaffold: A synergistic bio-composite for wound healing. European Journal of Pharmaceutical Sciences, 52, 26–33. https://doi.org/10.1016/j.ejps.2013.10.006.

Rather A.H., Wani T.U., Khan R.S., Pant B., Park M., Sheikh F.A. (2021). Prospects of polymeric nanofibers loaded with essential oils for biomedical and food packaging applications. International Journal of Molecular Sciences, 22, 12-28. https://doi.org/10.3390/ijms22084017.

Thenmozhi S., Dharmaraj N., Kadirvelu K., Kim H.Y.(2017). Electrospunnanofibers: New generation materials for advanced applications. Materials Science and Engineering B: Solid-State Materials for Advanced Technology, 217, 36–48. https://doi.org/10.1016/j.mseb.2017.01.001.

Thakur R.A., Florek C. A., Kohn J., Michniak B.B. (2008)Electrospunnanofibrous polymeric scaffold with targeted drug release profiles for potential application as wound dressing. International Journal of Pharmaceutics, 364, 87–93. https://doi.org/10.1016/j.ijpharm.2008.07.033.3,

Tanrıverdi S.T., Suat B., Azizoğlu E., Köse FA., Özer Ö.(2018). In-vitro evaluation of dexpanthenol-loaded nanofiber mats for wound healing. Tropical JournalofPharmaceutical Research, 17, 387–394. https://doi.org/10.4314/tjpr.v17i3.1.

Tas C., Ozkan Y., Okyar A., Savaser A. (2007). In vitro and ex vivo permeation studies of etodolac from hydrophilic gels and effect of terpenes as enhancers. Drug Delivery, 14, 453–459. https://doi.org/10.1080/10717540701603746.